Strength Criteria for Rock masses with Gouge Filled Discontinuities

U.N. Sinha
Geotechnical Engineering Division
Central Building Research Institute
Roorkee - 247 667, India
E-mail: general@cscbri.ren.nic.in

Bhawani Singh
Department of Civil Engineering
University of Roorkee, Roorkee - 247 667, India
E-mail: civil@rurkiu.ernet.in

ABSRACT

Rock masses near slopes behave as discontinuum due to the presence of discontinuities such as joints, faults, shear zones, thrust zones, bedding planes, etc. The stability depends on the geometry of discontinuities and the slope and orientation of excavated face. The most important factor is the shear strength of potential failure planes. The characterisation of a discontinuity or a shear zone is not possible merely by looking at a specimen or by subjecting to conventional laboratory testing. The genesis of shear zone, its stress-strain history, the strength-deformation relationship, the degree of particle parallelism and compression texture of shear zone, all combined to modulate its behaviour particularly when it approaches the state of limit equilibrium. Based on extensive experimental results, it was found that the deviator stress which controls the shear failure is a better criterion for evaluating shear strength of joints with thick gouge (t>>a). As such, on the basis of unconsolidated undrained (U-U) triaxial tests, authors suggested a strength criteria for rock masses with gouge filled discontinuities.

1. INTRODUCTION

Rock masses are discontinuous and their instability depends on the geometry of discontinuities and the slope and orientation of excavated face. The most important factor is the shear strength of potential failure planes. The strength and deformational behaviour govern rock mass failure mechanism when it approaches the state of limit equilibrium.

The presence of discontinuities in a rock mass not only decreases the ultimate strength of the rock but also makes it more deformable and permeable. This ultimately affect the engineering behaviour of the rock mass. In addition to the stress conditions, the geometry of the discontinuity surface (undulating/planar) also plays an important role in influencing the engineering behaviour of the rock mass [Sinha (1993), Sinha and Singh (1989)].

Tight rough joints with interlocking asperities increase the strength and stiffness of the rock mass even at low normal stress. When joints are filled with some materials having strength lower than the host rock, the joint properties influenced by the properties of the filled material. It is reported that the choice of the correct shear parameters is difficult in the case of joints in relatively hard rock filled with weak and loose material varying from coarse gouge to sand to clay and constituting either shear debris and highly weathered products of rock material or deposited erosion products [Lama (1978), Lama and Vutukuri (1978), Kutter and Rautenberg (1979), Hassani and Scoble (1985), Papaliangas et al. (1993)].

The filling materials, often termed as gouge, may be in the form of partially loose to completely loose cohesive and non-cohesive weathered material and is deposited in open joints, shear zonez, faults, etc. The thickness of the fill material may vary from a fraction of a micron to several millimetres. In case of tectonically crushed rocks the thickness of filling or gouge may increase up to several meters. Any clayey gouge in a sloped discontinuity makes the rock mass more prone to instablity. When such a gouge becomes wet, it promotes sliding of the rock blocks.

Barton (1974) has also made an extensive review of the shear strength of filled discontinuities in rock. It is reported that the shear strength of joints with thick layer of filling is almost similar to the strength of filler. The strength and stiffness of infilled joints change gradually with the relative filler thickness and an influence of the surface roughness exist even for thicker fills (Kutter and Rautenberg,1979).

Various workers have directed investigations on artificially created joints in rocks. However, study of development of pore water pressure during shearing, the influence of gouge thickness on strength of joint with dip of discontinuity surface have not been taken up in such investigation (Sinha and Singh, 1996).

As such, the study was undertaken to observe the behaviour of clayey gouge material along discontinuity surfaces in rock mass. The materials retrieved from the actual discontinuities and the materials ambient to it was studied under unconsolidated undrained (U-U) condition at various strain rates, thickness and dip angles both for undulating and planar surface profile in laboratory using computer controlled triaxial testing system. Need is felt to extend Barton's

equation to assess and predict the shear strength of discontinuity surfaces of rock mass filled with clayey gouge.

A new shear strength criterion of joints filled with gouge after modification of Barton's equation was developed on the basis of extensive experimental data for slope stability analysis, foundation problem and analysis for underground opening (Sinha, 1997).

2. LANDSLIDE SITE, GOUGE MATERIAL AND PROPERTIES

2.1 Geology of Landslide Site

Kaliasaur landslide is located on Rishikesh-Badrinath road at about 18 km east of Srinagar (Garhwal) (Fig. 1). The landslide occurred in the Garhwal group of rocks. The main rocks in the area are white and greenish quartzites interbedded with maroon shales. Observations along the road and the river Alaknanda suggest the presence of two types of quartzites. One is of green colour with thin beds of maroon shales and other is massive and well jointed yellowish white quartzites. On the western side of the slide zone, the quartzites are light green with shale bands having a general southward dip ranging from about 25° to 60°. These exposures are separated by a scree zone beyond which massive yellowish quartzites dipping southeast at 30°- 40° are exposed. On the eastern side of the slide zone, the exposed quartzites have interbedded maroon shales with southeasterly dip of 30°-40°.

The morphometric parameters indicate the presence of planar type of failure showing flow of debris on down slope without creating any deep seated failure through bed rocks. Kaliasaur landslide is essentially a multi-tier retrogressive landslide in a complex rock formation subjected to faulting and intense tectonic activity in the geological past. Evidences of sliding and crumbling of maroon shales along their boundaries with quartzite bands were observed (Bhandari, 1987; Sinha, 1993).

2.2 Gouge Material

Samples of gouge materials (shales) were collected from joints and other discontinuities (Figs. 2 and 3) to study their properties and shear strength characteristics of shear zones and slip surfaces both for undulating and planar joints in undrained condition. The gouge materials collected were pulverised in mortar and pestle till all materials passed through 425 microns of Indian Standard sieve without rejecting any residue retained on 425 microns sieve. It was done to simulate pulverisation of the shale into gouge material of homogeneous mineralogical compositions as present in field situation.

2.3 Physical Properties

The liquid limit (LL) and plasticity index (PI) were determined and they were found in order of 24-26% and 5-6% respectively. Silt and clay contents were 46.9% as obtained on analysis by washing through 75 microns Indian standard sieve. The gouge material indicated clay of low plasticity.

2.4 Chemical Analysis

Two samples of gouge material from different discontinuities were collected for chemical analysis and the results are given in Table 1 (Sinha, 1993; Sinha and Singh, 1996).

Table 1: Results of chemical analysis of gouge material

Major Oxides (%)	Sample 1	Sample 2
SiO_2	57.08	59.55
Al_2O_3	15.04	27.26
Na_2O	4.34	0.32
MgO	4.09	2.16
P_2O5	0.42	0.10
K_2O	1.62	0.77
CaO	7.85	0.01
TiO_2	0.54	0.66
MnO	0.04	0.03
Fe_2O_3	4.97	5.77

2.5 XRD and DTA

XRD and DTA were also carried out. XRD analysis showed the presence of kaolinite mineral as accessory component associated with the bulk of sample. DTA revealed strong endothermic reactions in the temperature range 70-100°C and 550-600°C due to loss of mechanical and chemical water respectively. It was followed with an exothermic reactions in the temperature range of 90°-94°C due to formation of high temperature phases showing mica group of clay minerals. The presence of kaolinite group clay mineral as accessory was supported by XRD, DTA and chemical analysis (Sinha, 1993; Sinha and Singh, 1996).

3. TESTING METHOD

The perspex blocks of 38 mm diameter to maintain 76 mm height after filling the joints with the gouge material were fabricated with the provision of 2mm

diameter hole to saturate the filling material by applying back pressure and to measure pore water pressure during shearing. Undulating and planar type of joints were fabricated (Fig. 4) with dip angles as 5°, 20°, 30°, 45° and 50°.

The weighed quantity of gouge material was taken (art. 2.2) and water is added to it. After thorough mixing the gouge is ready to fill. The test specimens were, then prepared for different thickness of gouge at pre-decided dip angles. The minimum thickness of gouge has been kept as 5mm, whereas the maximum thickness varies between 15 and 40mm with the dip angle. The test specimens were saturated by applying back pressure following saturation ramp procedure and unconsolidated-undrained tests were carried out at different speed of shearing (e), i.e. 5, 10, 20, 40 and 80 mm/hr. Computer controlled triaxial testing system was used for the tests (Fig. 5).

The data obtained from the above tests were plotted for analysis and results. Various plots are - normalised undrained strength vs speed of shearing (Figs. 6 a & b); effective angle of internal friction vs speed of shearing (Figs. 7 a&b); differential pore water pressure vs gouge thickness (Figs. 8a&b); pore water pressure factor vs gouge thickness (Figs. 9a&b); pore water pressure factor vs dip angle (Figs. 10a&b); differential axial stress vs dip angle (Figs. 11a&b); experimental and theoretical strength using Barton's equation (Figs. 12 a&c); correction factor f(t/a) vs t/a (Figs. 13 a&b) shear modulus vs t/a (Figs. 14 a&b).

4. INTERPRETATION OF RESULTS

4.1 Effect of Speed of Shearing

There are conflicting observations on the effect of the speed of shearing (e) on the shear strength behaviour of filled discontinuity surfaces. That is why a series of unconsolidated-undrained (U-U) tests were carried out at various speed of shearing (5 to 80 mm/hr). The effect of speed of shearing on normalised effective angle of internal friction was not found to be significant at any dip angle (Figs. 7a&b). However, effect of speed of shearing on normalised undrained shear strength (Figs. 6a&b) revealed decrease in strength for speed of shearing from 20 to 40 mm/hr and thereafter the increasing trend was observed. The variation in trend was also noted. The present study suggests to carry out the test at controlled rate of strain as also suggested by Hassani and Scoble (1985) and Sinha (1993).

4.2 Development of Pore Water Pressure and Pore Water Pressure Factor

Figures 8(a&b) show the plot between differential pore water pressure and thickness and indicate an interesting behaviour in development of pore water

pressure with various thickness of gouge. The increasing trend of pore water pressure within the range of 5 to 20 mm gouge thickness and then decreasing trend upto 30 mm thickness and thereafter again increasing trend was observed for the dip angles from 30° to 50°. This indicates that the development of higher pore water pressure beyond 30° dip angle may reduce the effective stress resulting in reduction in strength. The effect of thickness of gouge in pore water pressure factor (r_u) also revealed interesting results at lower dip angle of 5° (Figs. 9 a&b). The pore water pressure factor was found to increase upto 20 mm thickness and then decrease upto 30 mm thickness and thereafter again increase drastically. However, beyond dip angle of 20° the increasing trend of pore water pressure factor up to 20 mm thickness was observed and thereafter marginal increase was seen indicating arriving at residual condition. The increase in pore water pressure factor was observed upto the dip angles of 30° to 35° and thereafter decrease and again sign of increase was seen (Figs. 10 a&b). This indicates maximum reduction in strength with the dip angles as mentioned above.

The extensive experimental results indicated the influence of the thickness and the dip angles on shear strength both for undulating and planar type of joints.

4.3 Effect of Dip Angle on Strength

The differential axial stress vs dip angle plots (Figs. 11a&b) revealed the decreasing trend and all curves for various thickness of gouge were found merging within the dip angles of 30° to 50°. The behaviour as observed agrees with the finding of other researchers (Donath, 1963; Bamford, 1969; Akai et al., 1970; Hoek, 1983; Ramamurthy, 1985; Arora and Trivedi, 1992; Sinha, 1993). It is interesting to note that there was no effect of speed of shearing for joints with dip angles 30° to 50° filled with gouge material whether undulating or planar, the shear strength is found to be the lowest within the range of dip angles 30° to 45°.

4.4 Influence of Gouge Thickness

At low dip angle, i.e., 5° to 20° in case of undulating joints no failure occurred even when the gouge thickness was 40 mm. Similar trend was observed in case of planar joints showing lower magnitude of deviator stress. It indicates that the effective angle of internal friction of joint is more than 20°. Significant influence of thickness on deviator stress in case of dip angles ranging from 20° to 50° for undulating type of joint was observed. The influence of thickness on deviator stress for planar joints was observed for lower thickness, i.e., t = 10 mm and beyond it this trend disappeared. This behaviour was in agreement with the work of other researchers (Goodman, 1970; Skempton, 1964 & 1985). It reveals the failure mechanism of filled discontinuities at low normal stress for predicting shear strength behaviour of rock joints filled with gouge in triaxial test.

5. MODIFICATION IN BARTON'S EQUATION

5.1 Transcendental Equation

Based on experimental results the plots between experimental maximum shear stress $(\sigma_1-\sigma_3)/2$ and the theoretical shear stress calculated on the basis of Barton's equation given below (Barton, 1974; Barton and Choubey, 1977) were plotted and and are shown in Figs. 12 a&c.

$$\tau = \sigma_n \tan\left[\text{JRC}\log_{10}\frac{\sigma_1-\sigma_3}{\sigma_n'} + \phi_b'\right] \quad (1)$$

where

τ	=	shear stress of fault or discontinuities
$\sigma'n$	=	effective normal stress at failure plane
JRC	=	Joint roughness coefficients
JRC	=	0 for smooth clean joint surface
JRC	=	20 for rough or undulating surface
$\sigma_1-\sigma_3$	=	deviator stress
ϕ'_b	=	basic frictional angle
if σ_3	=	0 the equation will have the same form of Barton's equation of rough clean joint, and

$$\tau = \sigma_n' \tan\left[\text{JRC}\log_{10}\frac{\text{JCS}}{\sigma_n'} + \phi_b'\right] \quad (2)$$

Where,

JCS = Joint wall compressive strength.

The dip angles for undulating joints were modified because no clear failure surface was observed. However, in case of planar joints the failure took place on the surface due to slippage clearly. As can be seen it revealed linear relationship and majority of points were found very close to unity line for modified, unmodified, undulating and planar joints filled with gouge with a slight upward trend beyond dip angles of 30°. This provided an insight to incorporate modification in Barton's equation mentioned above to predict the shear strength for the filled discontinuities considering different dip angles. This indicated to derive the following transcendental equations for undulating and planar joints for predicting the strength of thick gouge (t/a > 1.25 thickness amplitude ratio).

$$\tan \phi_i = \sin 2\beta \tan\left[JRC \log_{10} \frac{\tan \phi_j'}{\sin 2\beta} + \phi_b' \right] \quad (3)$$

where,

$\phi'j$ = frictional angle of joint filled ith gouge

β = dip angle (angle between joint plane and major principal plane)

The transcendental equation for planar joint may directly be derived by putting JRC = 0 for predicting strength of joint filled with gouge i.e.

$$\tan\phi_i = \sin 2\beta \tan \phi'_b \text{ - planar joint (condition } \tan\phi'j = \tan \phi'b \text{)}$$

when thickness will be large, i.e., t>>a, ϕ'_b is equal to sliding angle of friction along contact plane between the gouge and surface of the host rock (Perspex used as dummy rock for the study).

The transcendental equation derived for planar joint assuming, JRC = 0 is proposed and suggested to predict the shear strength criteria. This type of situation will seldom be present in actual field conditions. However, it can be utilised in case of development of residual strength in post-failure condition similar to cut-plane for low thickness encountered due to large movement.

5.2 Correction Factor

In the Eq. 3 the factors such as joint roughness (JRC), orientation of joint (dip angle), asperities, pore water pressure and basic effective friction angle (ϕ'_b) are already covered excepting function of thickness-amplitude ratio [f(t/a)]. The following equations were used to evaluate the correction factor [f(t/a)].

$$f(t/a) = \left[\frac{\tan \phi_j'}{\sin 2\beta \tan(JRC \log_{10}) \frac{2 \tan \phi_j'}{\sin 2\beta} + \phi_b'} \right] \quad \text{Undulating} \quad (4)$$

$$f(t) = \left[\frac{\tan \phi_j'}{\sin 2\beta \tan \phi_b'} \right] \quad \text{Planar} \quad (5)$$

On the basis of calculated mean values of f(t/a) both for undulated and planar joints filled with gouge the relationship between f(t/a) and thickness amplitude ratio (t/a) were plotted [Fig. 13(a-b)].

The decreasing trend in f(t/a) was observed upto t/a = 10 by extrapolation and thereafter the decreasing trend was found whuch is insignificant. This was found much larger than suggested by Goodman (1970), Barton (1974) and Papaliangas et al. (1993) mostly carried out in direct shear box. In triaxial this condition may be possible. The nature of curve may be considered exponential. The correlation $f(t/a) = x + ye^{-t/a}$ was considered where x and y are material constants. On solution, the following correlations have been derived to apply correction factor (f) to the above transcendental equations are given below:

$$f(t/a) = 0.85 + 1.05\, e^{-t/a} \quad - \quad \text{Undulating joint} \qquad (6)$$

$$f(t) = 0.63 + 0.61 e^{-t/4} \quad - \quad \text{Planar joint} \qquad (7)$$

5.3 Prediction of Shear Modulus

The shear modulus were estimated from the plots between maximum shear stress and shear strain following initial tangent method. The normalised shear modulus (G/G_o) considering G_o was the lowest shear modulus corresponding to thick gogue material (if t>> a). Since the attainment of failure condition does not seem to be possible in case of lower dip angle ($\beta < 20°$), hence shear modulus for dip angle 5° was not considered to develop correlation for the prediction of shear modulus. The plots between normalised shear modulus (G/ G_o) and t/a ratio both for undulating and planar joints for unconsolidated undrained (U - U) test are shown in Figs. 14(a&b).

As can be seen, the variation and scattering in results due to variation in dip angles and roughness of joints are evident. Hence, the average curve drawn was observed exponential and the equation $G/ G_o = a + b\, e^{(-t/a)\tan\beta}$ was derived. The following correlations have been developed to predict shear modulus of discontinuities filled with gouge.

$$G/ G_o = 0.95 + 2.12\, e^{(-t/a)\tan\beta} \quad - \quad \text{Undulating joint} \qquad (8)$$

$$G/ G_o = 0.75 + 3.53\, e^{(-t/4)\tan\beta} \quad - \quad \text{Planar joint} \qquad (9)$$

5.4 A Simple Techniuqe for Assessing Strength

5.4.1 Shear and effective normal stress at failure plane

The magnitude of shear stress and effective normal stress at failure plane (Fig. 15) can be found from the following :

$$\tau = \frac{\sigma_1 - \sigma_2}{2} \sin 2\beta \qquad (10)$$

$$\sigma_n = \frac{\sigma_1' + \sigma_3'}{2} + \frac{\sigma_1 - \sigma_3}{2} \cos 2\beta \qquad (11)$$

$$\phi_j' = \tan^{-1}\left(\frac{\tau}{\sigma_n}\right) \qquad (12)$$

$$\tan \phi_j' = \left(\frac{\tau}{\sigma_n}\right) \qquad (13)$$

where,

σ'_1	=	effective axial stress
σ'_3	=	effective cell pressure
β	=	angle between joint plane and major principal plane (designated as dip angle)
τ	=	shear stress at failure plane
σ_n	=	effective normal stress at failure plane

5.4.2 Modification in dip angle, shear and normal stresses at modified failure plane

It was observed that the failure pattern of undulating (rough) joint filled with gouge was not found to follow the plane inclined at the joint dip angle. The filled joint showed deformation and squeezing (bulging out) of the gouge material along the undulating surface (Fig. 16) necessitating modification of dip angle. The failure of joint filled with gouge in case of planar profile (smooth type) showed the failure exactly through the pre-determined failure angle, i.e., dip (Fig.17). Hence, the modification in case of planar joint was not found necessary (Fig. 18).

The modification as incorporated in case of undulating joint surface is illustrated in (Fig. 19).

On evaluation of modified dip angle, the magnitude of shear stress and effective normal stress at modified failure plane can again be determined from the following relationships.

$$\tau_m = \frac{\sigma_1 - \sigma_3}{2} \sin 2\beta_m \qquad (14)$$

$$\sigma'_{n(m)} = \frac{\sigma'_1 + \sigma'_3}{2} + \frac{\sigma_1 - \sigma_3}{2} \cos 2\beta_m \qquad (15)$$

$$\phi'_m = \tan^{-1}\left(\frac{\tau_m}{\sigma'_{n(m)}}\right) \qquad (16)$$

5.4.3 Prediction of strength

The failure mechanism of undulating and planar joints filled with gouge mainly depends on the discontinuity surfaces, thickness of fill material (gouge), orientation of joint,i.e., dip angle, drainage condition, test condition and type of equipment. Figures 20 a&b show plots between effective modified angle of internal friction and modified dip angle and effective angle of internal friction (modified) and dip angle (unmodified for undulating joints) respectively. Figure 21 shows the plot of unmodified effective angle of internal friction and dip angle for planar joints.

The results were found scatter showing the influence of thickness and speed of shear. However, a bilinear curve fit was found to predict the shear strength at any particular dip angle for quick assessment. Since the stage of failure below dip angle 20° was not found critical to achieve, the bilinear curve beyond 20° may be considered for assessing shear strength criteria. The following equations may be used to predict shear strength criteria for rock slope stability and foundation problems on discontinuous rock mass carried out for unconsolidated undrained condition in triaxial.

$$\tan \phi'_j = 17° + \beta \tan 10.2° \text{ - Undulating joint} \qquad (17)$$

$$\tan \phi'_j = 12° + \beta \tan 7.6° \text{ - Planar join} \qquad (18)$$

6. CONCLUSIONS

Based on experimental results the following conclusions are offered:

- The deviator stress which controls the shear failure is a better criterion for evaluating shear strength of joints with thick gouge (t/a > 1.25).

- Accordingly modifications in equation proposed by Barton (1974) for evaluation of shear strength of rock joints have been made for rock joints filled with clay gouge (t/a > 1.25) considering unconsolidated undrained test in triaxial.

- The new strength criterion are suggested below for predicting shear strength of joints filled with gouge.

$$\frac{\sigma_1 - \sigma_3}{2} = \sigma_n' \, f \tan\left[JRC \log_{10} \frac{\sigma_1 - \sigma_3}{\sigma_n'} + \phi_b' \right] \quad \text{Undulating joint} \qquad (19)$$

$$\frac{\sigma_1 - \sigma_3}{3} = \sigma_n' \, f \tan \phi_b' \quad \text{Planar joint} \qquad (20)$$

where,

f = correction factor due to thickness of gogue (t/a)

$$f(t/a) = 0.85 + 1.05\, e^{-t/a} \quad \text{- Undulating joint} \qquad (21)$$

$$f(t) = 0.63 + 0.61 e^{-t/4} \quad \text{- Planar joint} \qquad (22)$$

- The simple techniques to assess shear strength [Figs. 20(a&b) and 21] are derived introducing dip effect.

$$\tan \phi'_j = 17° + \beta \tan 10.2° \quad \text{- Undulating joint} \qquad (23)$$

$$\tan \phi'_j = 12° + \beta \tan 7.6° \quad \text{- Planar joint} \qquad (24)$$

- The following correlations are developed to assess shear modulus of discontinuities filled with gouge.

$$G/G_o = 0.95 + 2.12\, e^{(-t/a)\tan\beta} \quad \text{- Undulating joint} \qquad (25)$$

$$G/G_o = 0.75 + 3.53\, e^{(-t/4)\tan\beta} \quad \text{- Planar joint} \qquad (26)$$

The magnitude of development of pore water pressure factor (r_u) during shearing may provide a tool to under take risk analysis in seismic hilly region.

Acknowledgement

The paper is published with the kind permission of the Director, Central Building Research Institute, Roorkee. Encouragement of Dr. R. K. Bhandari, Ex Director, CBRI is gratefully acknowledged. The first author would like to offer sincere thanks to Mr. S.N. Bhargava, Dr. Pradeep Kumar all of C.B.R.I for the help in preparing the paper. Thanks are also due to Mr. A.K. Mishra for the preparation of figures.

REFERENCES

1. Barton, N. (1974). A Review of the Shear Strength of Filled Discontinuities in Rock, NGI Publication 105, Oslo, pp. 1-48.
2. Barton, N., Choubey, V.D. (1977). The Shear Strength of Rock Joints in Theory and Practice, Rock Mechanics 10, pp. 1-54.
3. Bhandari, R. K. 91987). Slope Stability in the Fragile Himalaya and Strategy for Development, Ninth Annual Lecturem Indian Geotechnical Society, pp. 1-81.
4. Goodman, R.E. (1970). The Deformability of Joints and Determination of the Insitu Modulus of Deformation of Rock, Proc. Symp. Demer Colo, ASTM Spl. Tech. Paper 477, pp. 179-196.
5. Hassani, F. P. and Scoble, M. J. (1985). Frictional Mechanism and Properties of Rock Discontinuities, Proc. Int. Sym. On Fundamental of Rock Joints, Bjorkliden, Sept. 15-20, pp. 81-91.
6. Hoek, E. (1983). Strength of Jointed Rock Masses, Geotechnique 33, No. 3, pp. 187-223.
7. Kutter, H. K. and Rautenberg, A. (1979). The Residual Shear Strength of Filled Joints in Rock, Proc. 4th Symp. ISRM, Montreu, Vol. I, pp. 123-132.
8. Lama, R. D. (1978). Influence of Thickness of Fill on Shear Strength of Rough Rock Joints at Low Normal Stress, Grundlagan and Felsmechanik, Felsmechanik Kolloquium, Karlsruhe, Trans. Tech. Publ., Clausthal, pp. 55-56.
9. Lama, R.D. and Vutukuri, V.S. (1978). Handbook on Mechanical Properties of Rocks, Vol. 4, Chap. 10, Trans Tech. Publ.
10. Papaliangas, T., Hencher, S. R., Lumsden,A.C. and Manolopolon, S. (1993). The Effect of Frictional Fill Thickness on the Shear Strength of Rock Discontinuities, Proc. Int. J. Rock Mech. Min. Sci. & Geomech. Abstr., Vol 30, No. 2, pp.81-91.

11. Sinha, U. N. (1993).Behaviour of Clayey Gouge Material Along Discontinuities Surfaces, Ph. D. Thesis, UOR, Roorkee.
12. Sinha, U. N. (1994). Particle Breakdown due to Large Movement, Indian Geotech. J., Vol. 24, No. 3, pp.302-310.
13. Sinha, U. N. (1997). A New Strength Criteria of Discontinuous Rock Mass, Proc. IGC 97, Vadodara, pp. 113-116.
14. Sinha, U. N. and Singh, Bhawani. (1989). Undrained Shear Strength Behaviour of Artificially Created Shear Zone Material in Triaxial Test, Proc. Nat. Symp. On Application of Rock Mech. In River Valley Projects, Roorkee, Dec. 4-5, pp. 43-48.
15. Sinha, U. N. and Singh, Bhawani. (1996). Strength Prediction of Discontinuous Rock Mass, Proc. Int. Conf. On Recent Advances in Tunnelling Technology (RATT 96), March 18-20, New Delhi, pp. 23-40.
16. Skempton, A. W. (1964). Long Term Stability of Clay Slopes, Geotechnique 14, No. 2, pp. 75-102.
17. Skempton, A.W. (1985). Residual Strength of Cl;ay in Landslides, Folded Strata & the Laboratory, Geotechnique 35.
18. Ramamurthy, T. (1985). Stability of Rock Masses, 8th IGS Annual Lecture, IGC, Roorkee, pp. 1-74.

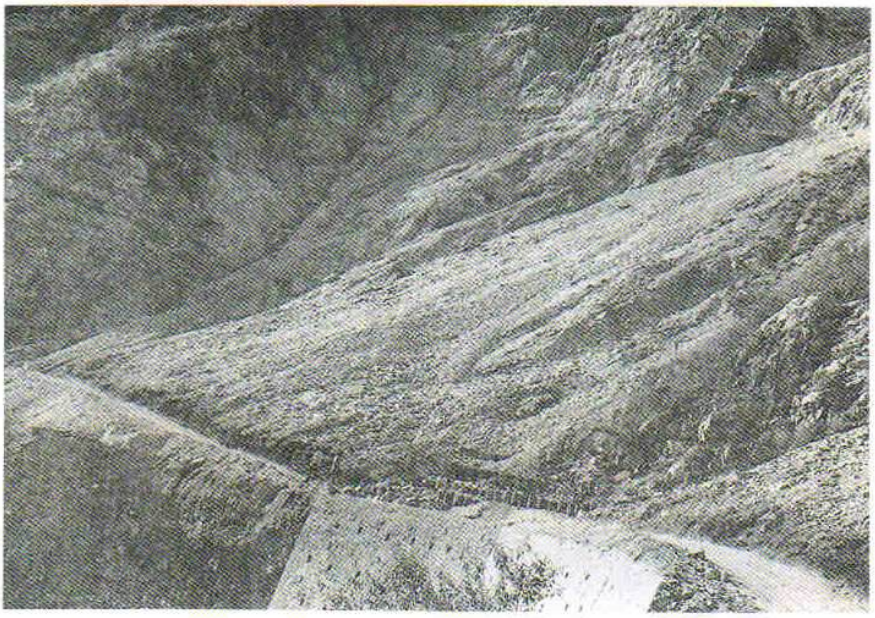

Figure 1: Landslide at Kaliasaur.

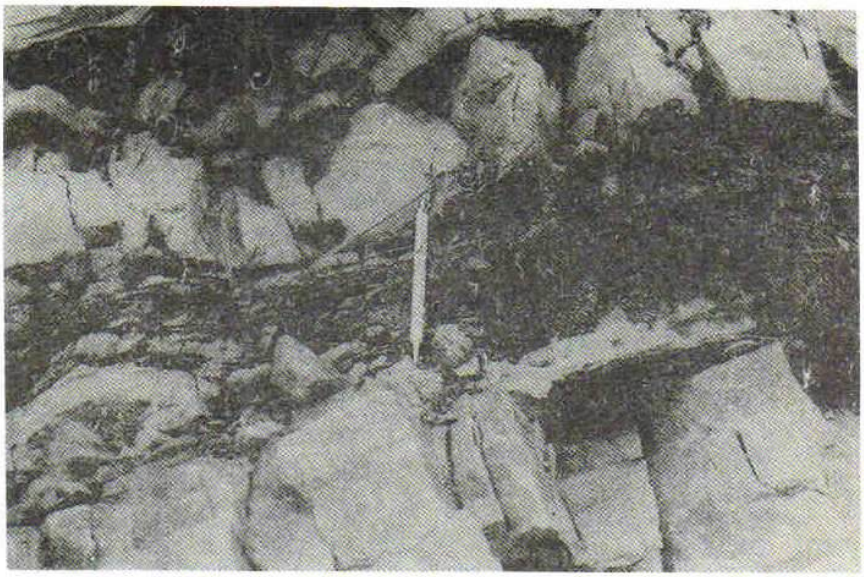

Figure 2: Presence of gouge material.

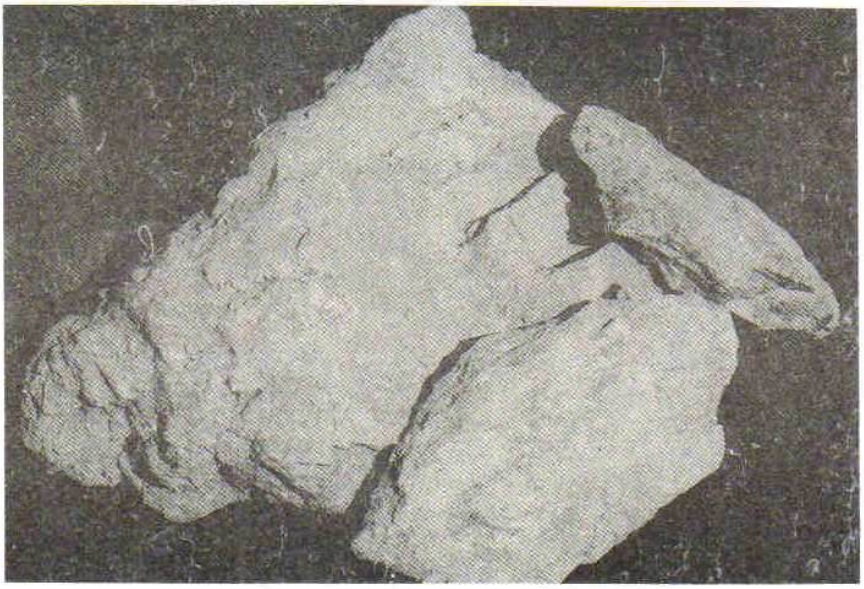

Figure 3: Gouge material.

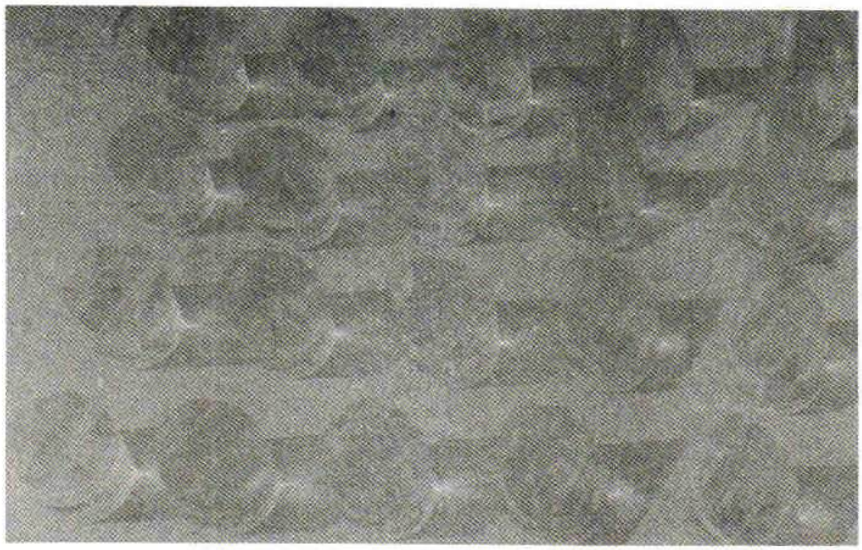

Figure 4: Fabricated undulating and planar joints

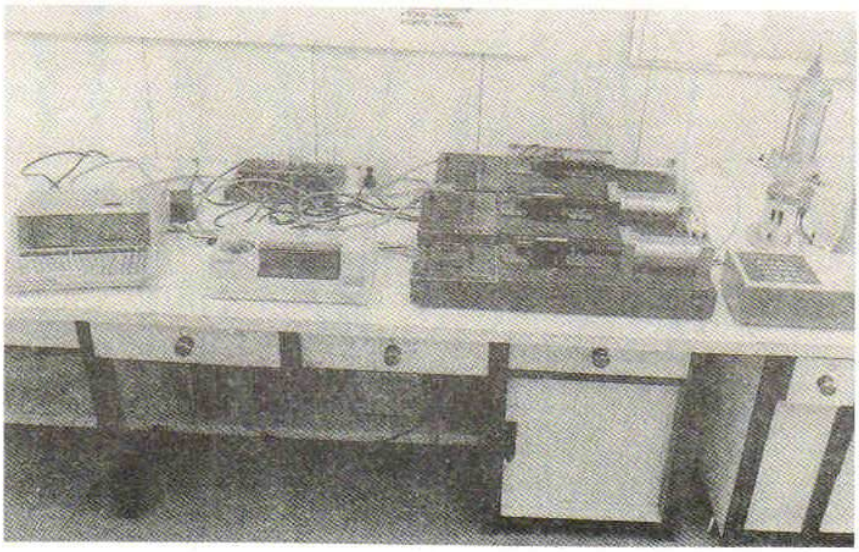

Figure 5: Triaxial testing system

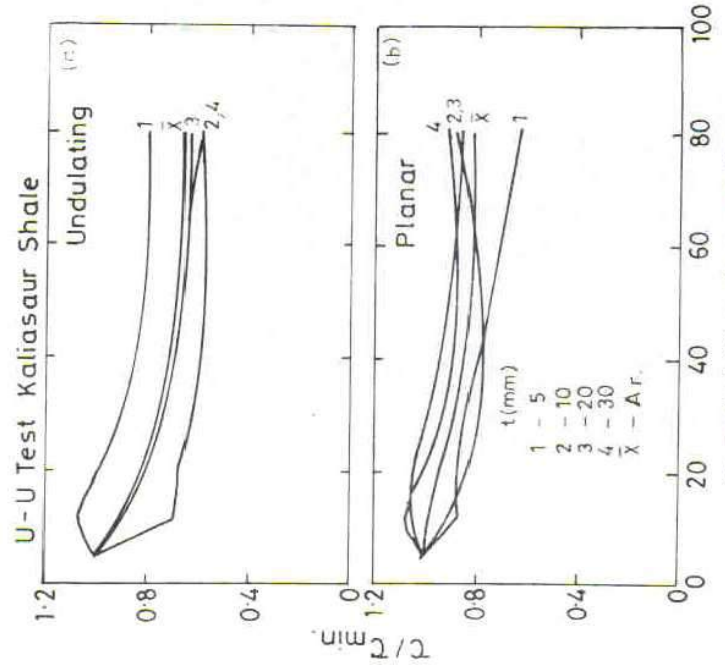

Figure 6 (a and b) : Normalised undrained strength Vs speed of shearing

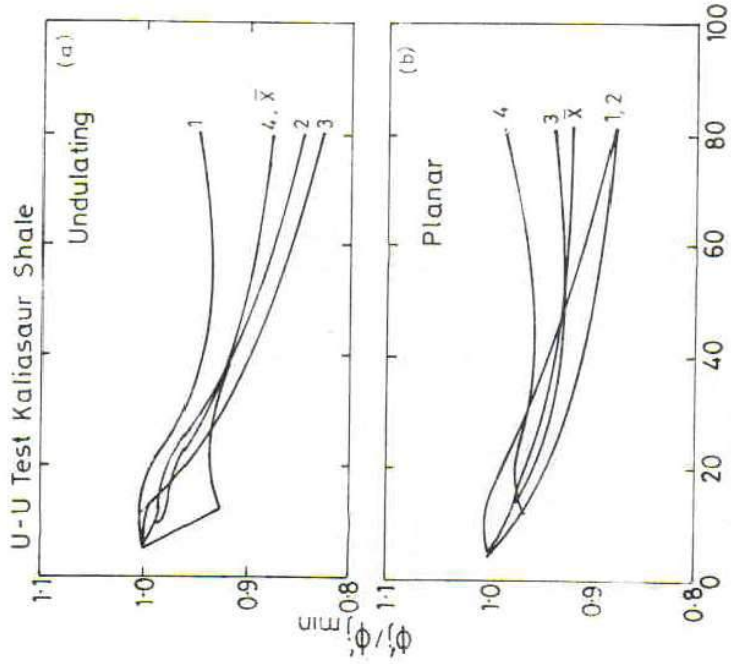

Figure 7 (a and b): Normalised effective angle of internal friction Vs speed of shearing

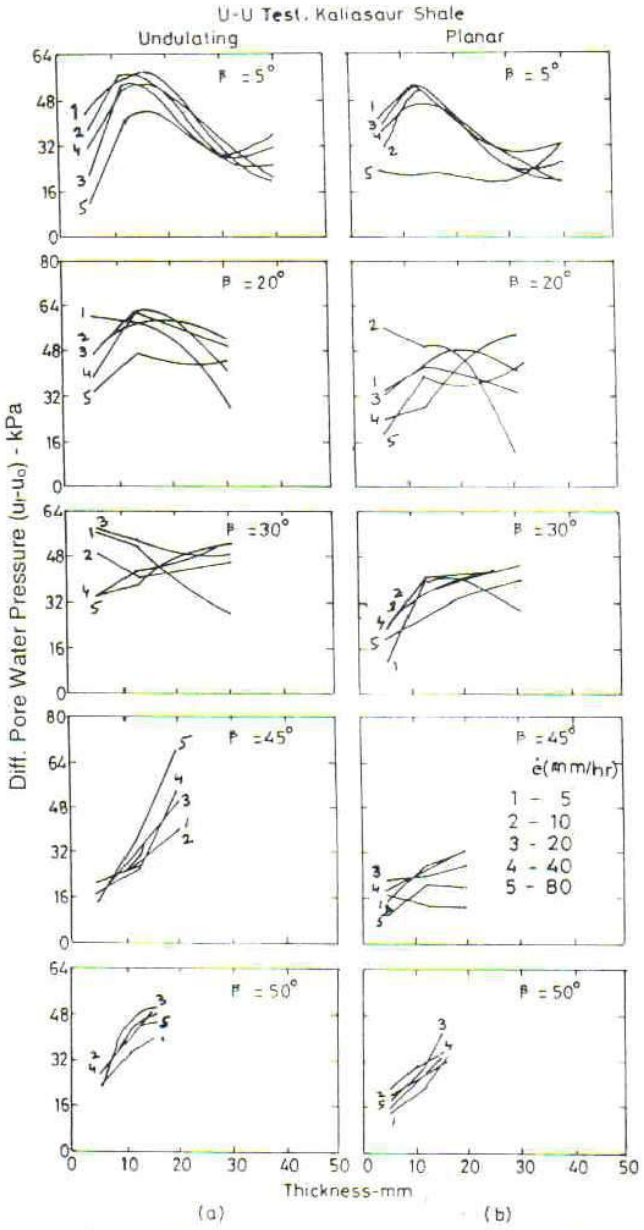

Figure 8 (a and b): Differential pore water pressure Vs thickness.

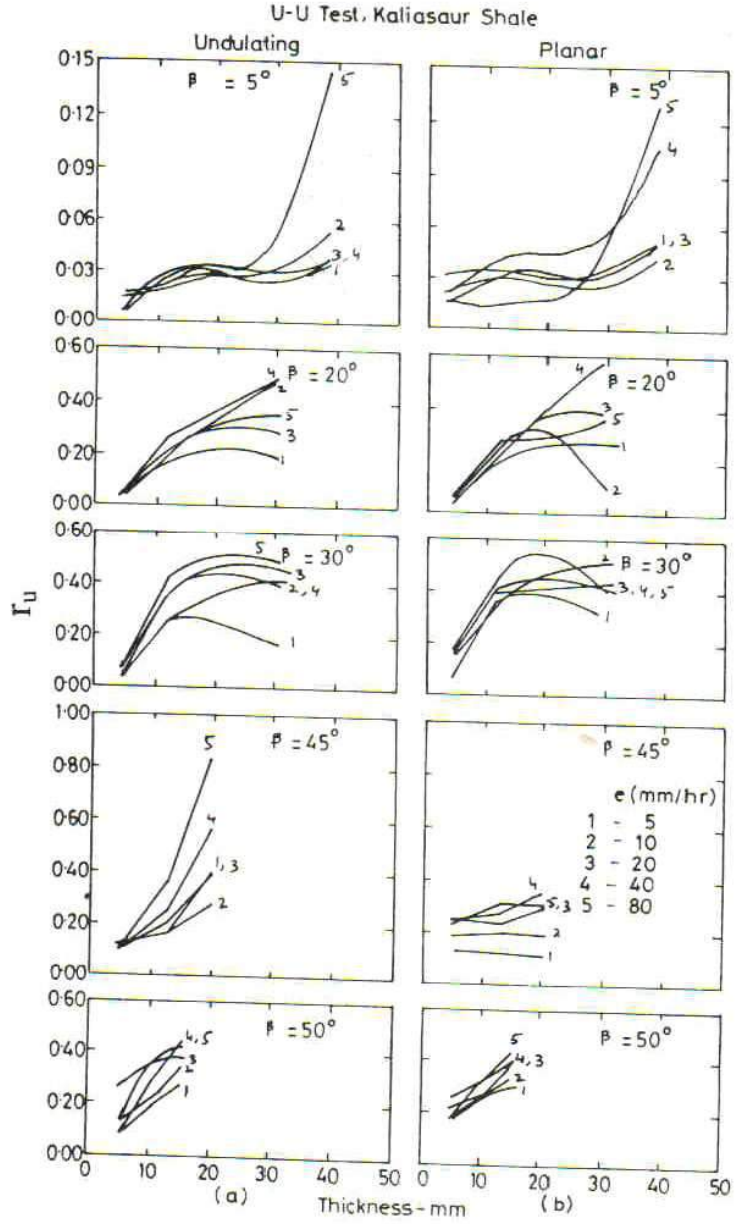

Figure 9 (a and b) : Pore water pressure factor Vs thickness.

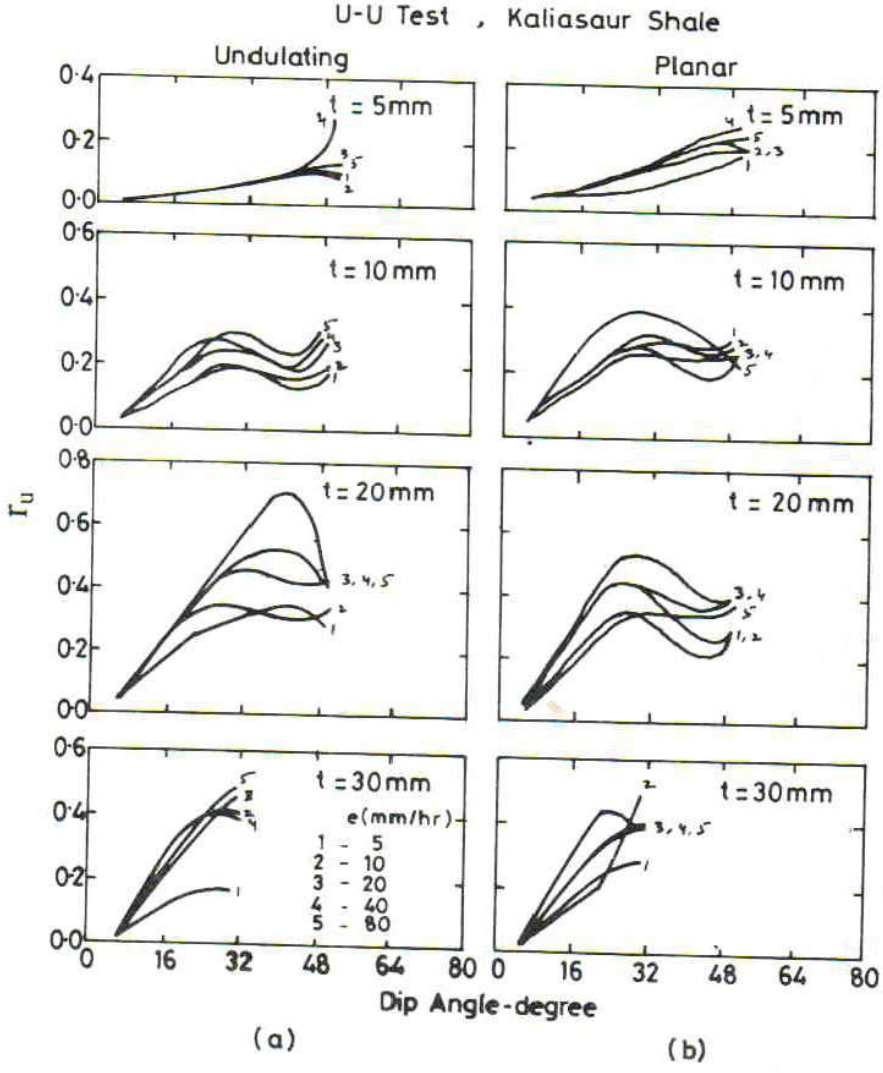

Figure 10 (a and b): Pore water pressure factor Vs dip angle.

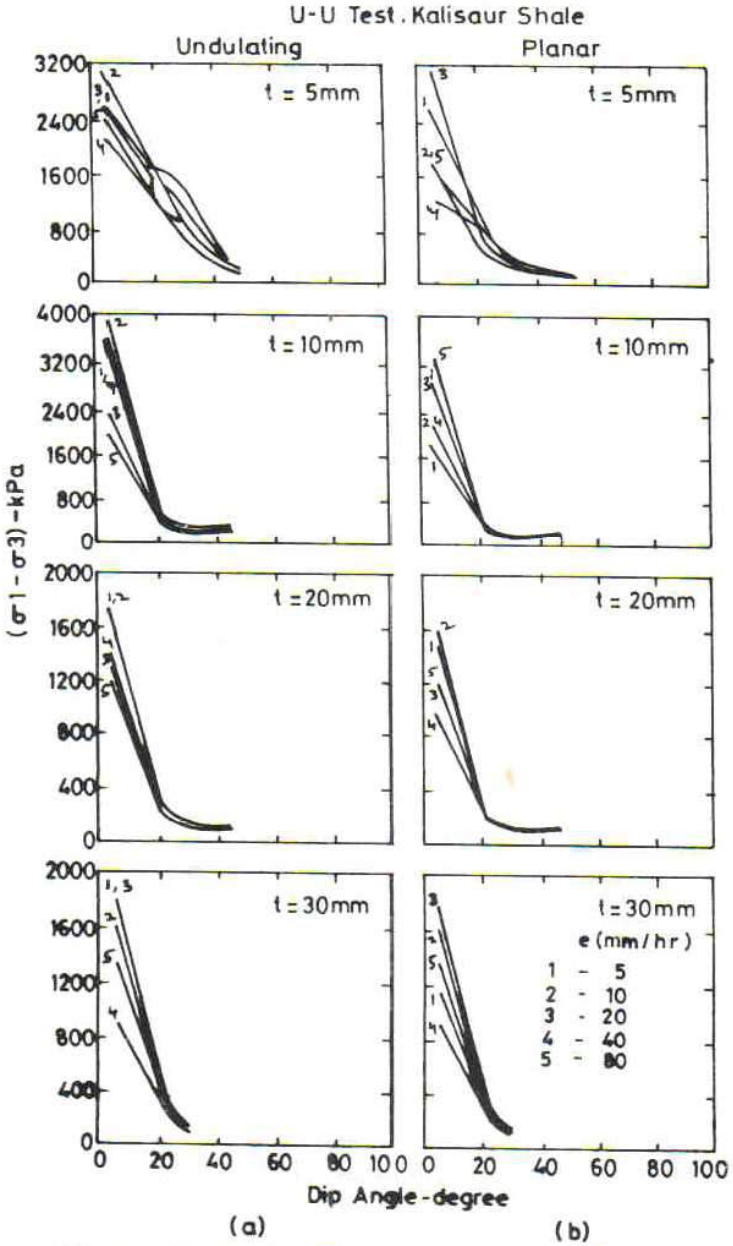

Figure 11(a and b): Differential axial stress Vs dip angle.

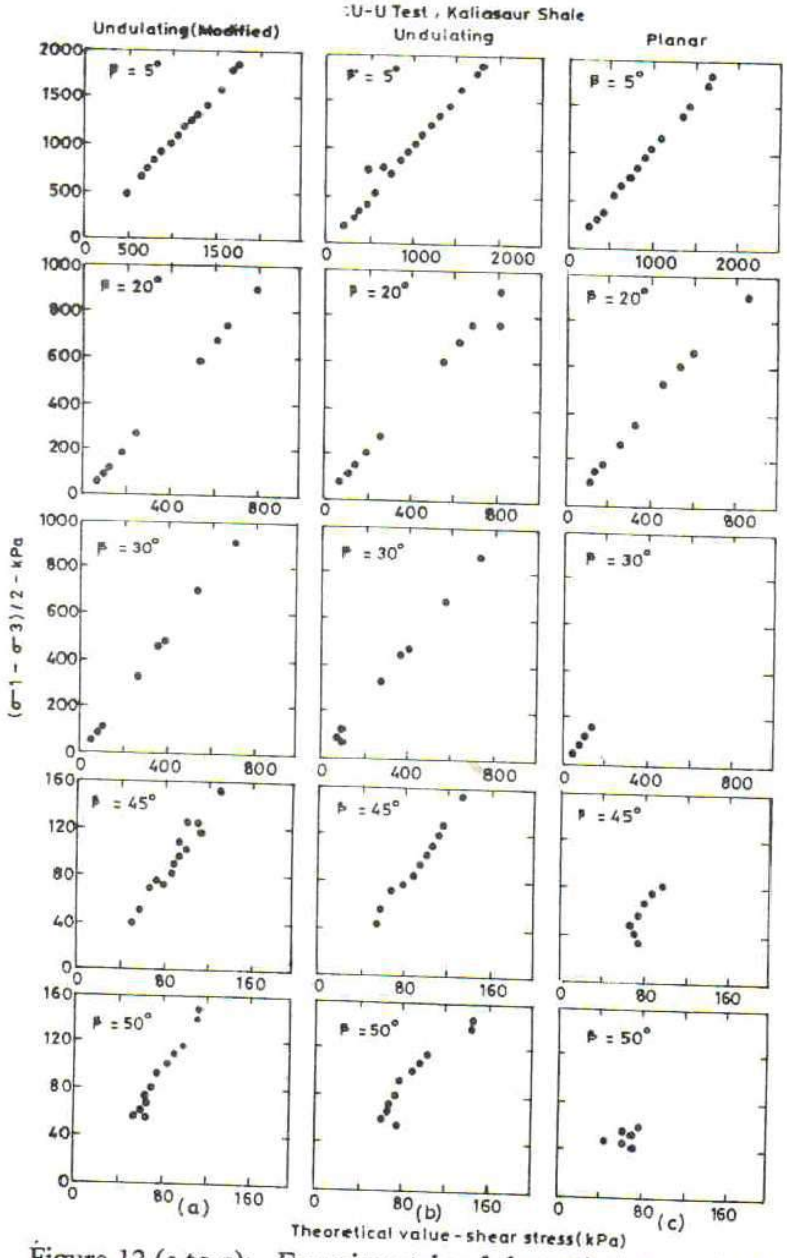

Figure 12 (a to c): Experimental and theoretical strength using Barton's equation.

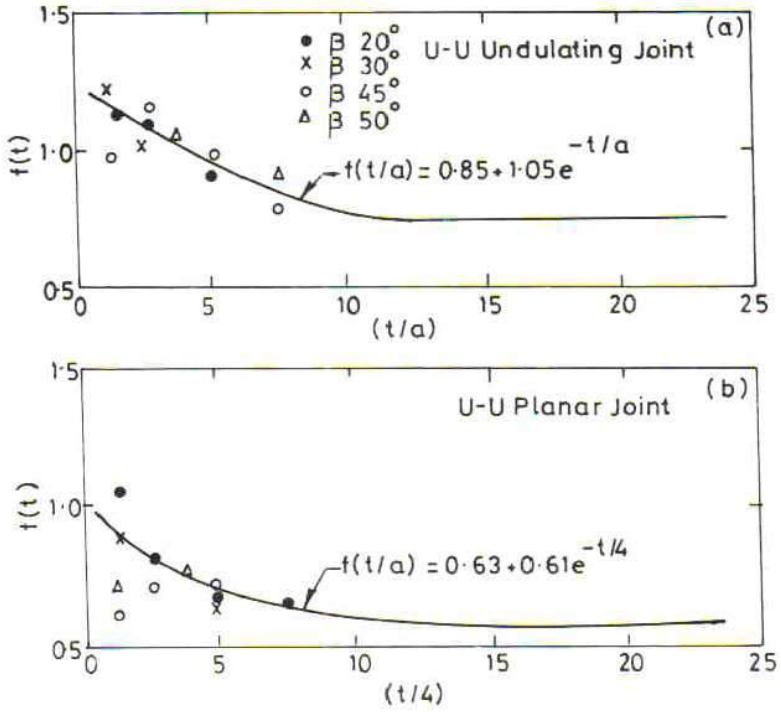

Figure 13 (a and b): Relationship between f (t/a) and t/a

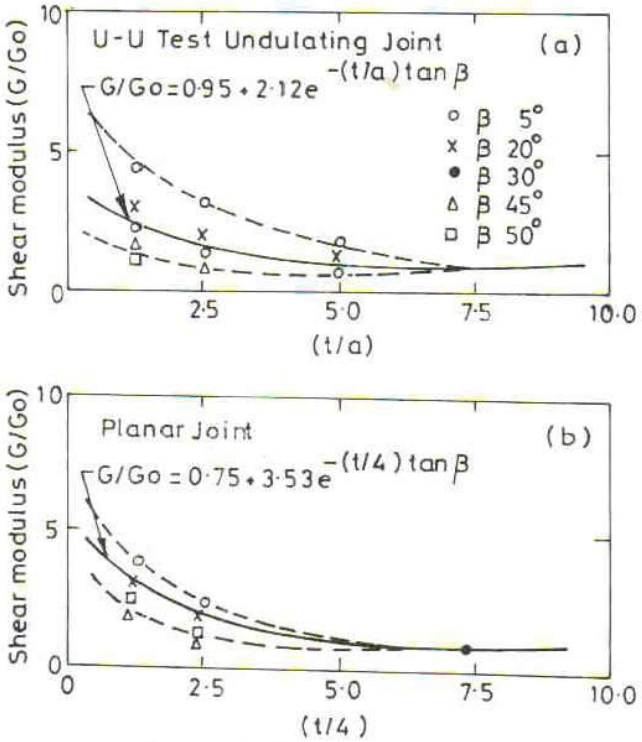

Figure 14 (a and b): Relationship between shear modulus and t/a

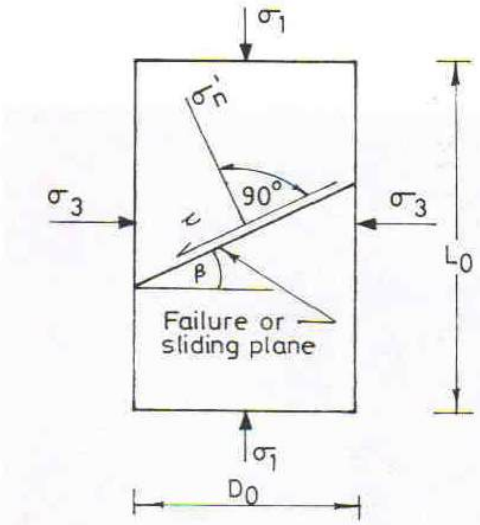

Figure 15: Shear and effective normal stress along failure plane

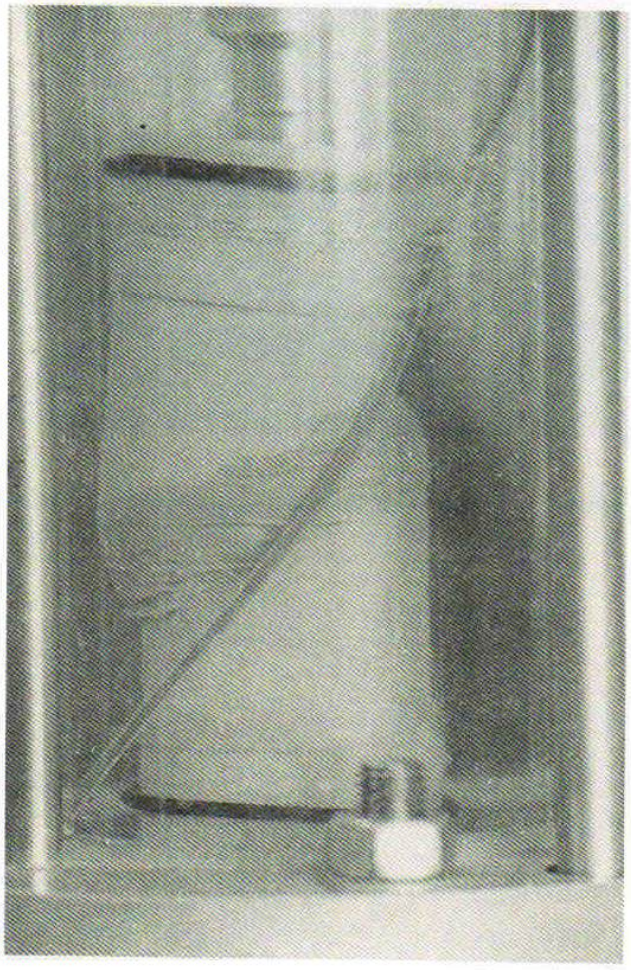

Figure 16: Undulating surface showing unclear failure plane

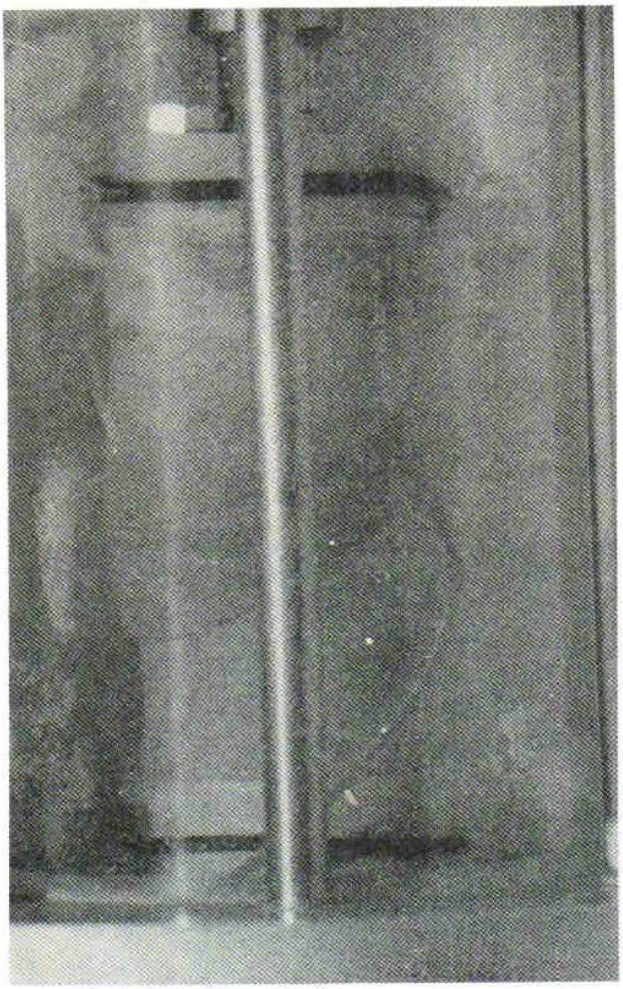

Figure 17: Planar surface showing clear failure plane.

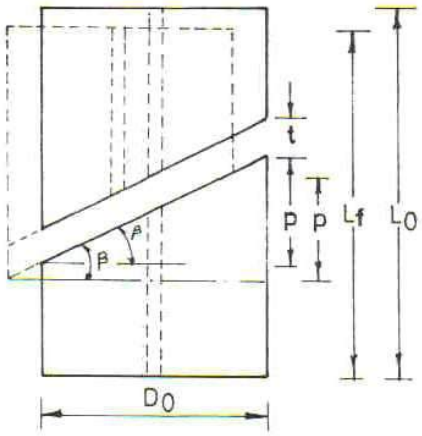

Non Modified Dip Angle
(Planar Joints)

Figure 18: Unmodification in dip angle for planar joint

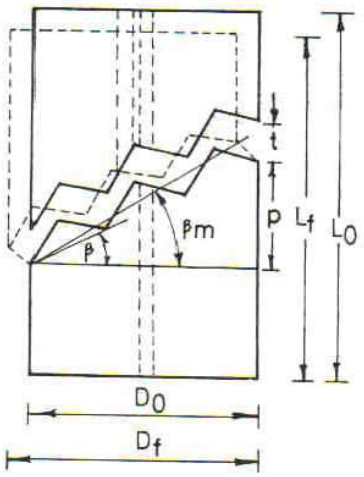

Modified Dip Angle
(Undulating Joints)

Figure 19: Modification in dip angle for undulating joint

L_o	=	Original length of test specimen
D_o	=	Original diameter of test specimen
D_f	=	Final change in diameter as recorded
L_f	=	Final change in length as recorded
t	=	Initial thickness of gouge material
β	=	Dip angle
p	=	$D_o \tan \beta$
βm	=	$\tan^{-1}(p+t/ D_f)$

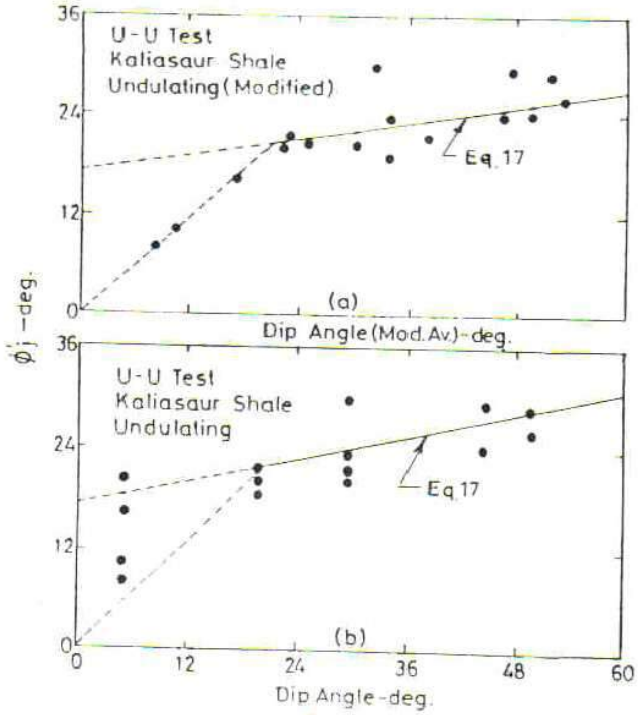

Figure 20 (a and b): Plot between effective angle of internal friction and dip angle (modified and unmodified dip angle for undulating joint).

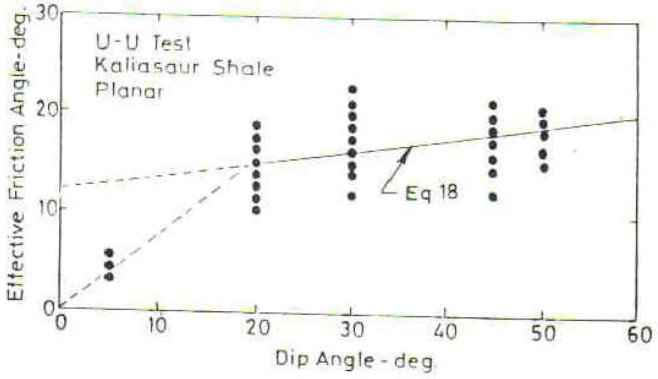

Figure 21: Plot between effective angle of internal friction and dip angle (planar joint).